KERNFORSCHUNGSZENTRUM

KARLSRUHE

April 1977 KFK 2429

Institut für Neutronenphysik und Reaktortechnik

Uranium borehole logging using delayed or prompt fission neutrons

G. Schulze, H. Würz

GESELLSCHAFT
FÜR
KERNFORSCHUNG M.B.H.

KARLSRUHE

GESELLSCHAFT FÜR KERNFORSCHUNG M. B. H.

KARLSRUHE

KERNFORSCHUNGSZENTRUM KARLSRUHE

KFK 2429

Institut für Neutronenphysik und Reaktortechnik

Uranium borehole logging using delayed or prompt fission neutrons

G. Schulze
H. Würz

Gesellschaft für Kernforschung mbH., Karlsruhe

Abstract

The measurement of induced fission neutrons is a sensitive method for an in situ determination of Uranium. Applying this methods requires a unique relation between concentration of Uranium and intensity of induced fission neutrons. A discussion of parameters influencing the determination of concentration is given. A simple method is developed allowing an elimination of the geochemistry of the deposit and of the borehole configuration.
Borehole probes using the methods described are of considerable help during the phase of detailed exploration of Uranium ore deposits. These on line tools allow an immediate determination of concentration. Thus avoiding the expensive and time consuming step of core drilling and subsequent chemical analysis.

Uranbestimmung in Bohrlöchern mit verzögerten oder prompten Spaltneutronen

Zusammenfassung

Die Messung induzierter Spaltneutronen gestattet einen empfindlichen in situ Nachweis von Uran. Eine Anwendung dieser Methode zur Uranexploration setzt allerdings voraus, daß eine eindeutige Zuordnung zwischen der Urankonzentration und der Intensität der induzierten Spaltneutronen besteht. Für die Methoden Messung der verzögerten Spaltneutronen und Messung der prompten Spaltneutronen werden die Parameter diskutiert, welche die Konzentrationsbestimmung beeinflussen. Eine einfache Methode zur Elimination der Einflüsse der Geochemie der Lagerstätte und der Bohrlochkonfiguration wird entwickelt.
Bohrlochsonden, die auf den beschriebenen Methoden basieren, stellen demnach ein attraktives Hilfsmittel bei der Detailerkundung der Ergiebigkeit von Uranlagerstätten dar. Der on line Betrieb der Sonden gestattet eine unmittelbare Konzentrationsbestimmung ohne den kostspieligen und zeitraubenden Umweg über Bohrkernerzeugung und nachfolgender chemischer Analyse.

Contents

1. Introduction

Due to the worldwide increasing number of nuclear power plants the demand for Uranium will increase considerably. According to Uranium market considerations /1/ the increasing demand for Uranium in the USA has to be met from reserves 80 % of which are potential reserves, that means these reserves still have to be found. During the next 10 - 15 years the Uranium supply will be met from Uranium deposits with typical ore grades around 0,2 % U_3O_3. Concerning the long range supply also lower grade ore in the range above 100 ppm U_3O_3 has to be explored and probably mined /2,3/.

Dealing with the increased Uranium demand the surface exploration activities have to be increased considerably. During 1975 total US borehole drilling amounted up to $7{,}8 \cdot 10^6$ m. The tendency is still increasing because of strongly decreasing amount of Uranium discovered per 1 m borehole drilled. These considerable drilling efforts are requiring fast methods for Uranium analysis. Most advantageous are in situ Uranium logging methods. These can be used in combination with simple percussion drilling. Reliable and sensitive methods for Uranium logging are developed. These methods are based on the measurement of the intensity of the neutron induced prompt or delayed fission neutrons (PFN or DFN respectively).

Borehole probes are in development using three different procedures /4-10/. These are i) measurement of delayed fission neutrons using a ^{252}Cf neutron source quickly removable from the irradiation position ii) measurement of delayed fission neutrons and iii) measurement of prompt fission neutrons. In these cases a pulsed 14 MeV neutron generator is used.

Zum Druck eingereicht am 13.4.1977

For all neutron induced methods the relation between the measurable intensity of induced fission neutrons and the Uranium concentration depends on local properties of the deposit. These may change considerably even within a single borehole. Therefore it is of great importance to know the influence of geochemical properties of a deposit on the determination of elemental concentration.

Recently some work has been reported on the problem of concentration determination in Uranium borehole logging /11-14/. Due to the very specific results great restrictions are imposed on the general applicability to different geological formations. The influence of neutron absorbers has only recently been discussed /14/.

In this paper a rather general treatment of concentration determination is given based partly on experimental results and on results of neutron transport calculations. The problems involved are similar to those encountered in borehole logging using the neutron induced gamma spectroscopy /15/. The good agreement between experiment and calculation in this case is demonstrating that a theoretical analysis is adequate for most practical cases.

2. Description of DFN and PFN method

Delayed fission neutrons(DFN) are emitted from several delayed neutron precursors produced from neutron induced fission in the Uranium isotopes ^{235}U and ^{238}U. Irradiation is performed either by using a periodically removed ^{252}Cf neutron source or by a 14 MeV neutron source which is switched on and off. The irradiation and timing conditions are depending on the half lives of the different delayed neutron precursors. Usually 6 groups of delayed neutron precursors are used /16/. Their halflifes and intensities are listed in table 1.

In case of the 14 MeV neutron source fission in ^{238}U contributes to the total amount of induced fissions and therefore also to the delayed neutron intensity. An additional source of delayed neutrons is the reaction $^{17}O(n,p)^{17}N$ having a threshold energy at 7.93 MeV.

Measurement of thermalized delayed fission neutrons is done using simple neutron counters such as BF_3 or ^3He detectors having a high sensitivity to thermal neutrons. The measurement starts as soon as possible after the end of irradiation waiting only until the thermalized source neutrons have died away.

In case of measurement of prompt fission neutrons (PFN) a pulsed 14 MeV neutron generator is used. Measurement of epithermal neutrons is done during a time interval of several msec. The measurement starts several 100 µs after the end of the neutron pulse. This method first was suggested by Czubek /9/. The induced prompt fission neutrons are showing the same exponential die away time behaviour as the thermalized source neutrons. The delayed neutrons contribute with a time independent fraction to the total countrate. Their contribution can be neglected if the measuring time interval is not made too large.

All three methods were considered. The detection limits obtainable with these methods are given in table 2. These data are taken from literature. The sources are indicated in the table. Due to the low detection limits borehole probes based on DFN or PFN are in principle a valuable tool in Uranium well logging.

3. Concentration determination for DFN

The steady state source neutrons (either ^{252}Cf spontaneous fission neutrons or 14 MeV neutrons) are slowed down and become finally thermalized in the Uranium containing rock thus producing a neutron flux distribution $\phi_1(\underline{r},E)$. Due to fission in both Uranium isotopes ^{235}U and ^{238}U the neutron flux at space point $\underline{r}$ causes a delayed fission neutron density distribution $S_D(\underline{r},E)$ according to:

$$S_D(\underline{r},E) = \frac{L}{A}C\chi(E)\left[R_f^{U38}(r)+R_f^{U35}(r)\right] = S_D^{U5}(\underline{r},E)+ S_D^{U8}(\underline{r},E) \quad (1)$$

with $\chi(E)$ energy spectrum of the delayed fission neutrons, is assumed to be the same for fission in U-235 and U-238

L Avogadro's number

A atomic weight

C concentration of Uranium

$$R_f^{U38}(r) = 0{,}9928\ \beta^{U8} \int \nu^{38}(E')\sigma_f^{38}(E')\phi_1(\underline{r},E')dE' \quad (2)$$

$$R_f^{U35}(r) = 0{,}0072\ \beta^{U5} \int \nu^{35}(E')\sigma_f^{35}(E')\phi_1(\underline{r},E')dE' \quad (3)$$

ν number of fission neutrons
σ_f fission cross section of isotopes U-235 and U-238
$\beta^{U5,U8}$ total delayed neutron fraction for U-235 and U-238

Converting $S_D^{U5}(\underline{r},E)$ and $S_D^{U8}(\underline{r},E)$ into the neutron fluxes ϕ_2^{U5} and ϕ_2^{U8} at the detector position r = 0 and taking into account the activation waiting and measuring time t_a, t_w, t_m respectively the relation between the concentration C of Uranium homogeneously distributed in the rock and the measured delayed fission neutron intensity CR in the borehole is given as

$$CR = C\left[CR(U8) + CR(U5)\right] \tag{4}$$

with $CR(U5,U8) = F^{U5,U8}(t)\int \varepsilon(E)\phi_2^{U5,U8}(O,E)dE$ (5)

and $$F^{U5,U8}(t) = \sum_{i=1}^{6} a_i^{U5,U8}(1-e^{-\lambda_i^{U5,U8}t_a})e^{-\lambda_i^{U5,U8}t_w}$$

$$\frac{1-e^{-\lambda_i^{U5,U8}t_m}}{\lambda_i^{U5,U8}} \tag{6}$$

describing the generation and decay of 6 groups of delayed neutron precursors.

$a_i^{U5,U8}$ relative abundance of delayed neutrons of group i for U5 or U8.

$\lambda_i^{U5,U8} = \frac{\ln 2}{T_{1/2\ i}^{U5,U8}}$ with $T_{1/2}^{U5,U8}$ halflife of group i

$\varepsilon(E)$ detector efficiency (proportional to 1/v for BF_3 and ^3He)

$\phi_2^{U5,U8}(O,E)$ neutron flux at detector position (r=O) due to delayed fission neutron density distribution $S_D^{U5,U8}(r,E)$.

Values for λ_i, a_i and β are listed in tables 1 a and 1 b.

The equations (5) and (6) are valid under the assumption that irradiation and subsequent detection of delayed neutrons are done at positions which are fixed during the respective times t_a, t_m.

In the theoretical treatment given the problem of determination of Uranium concentration reduces to two separate neutron flux calculational steps. In the first step the neutron flux ϕ_1 is calculated. From there the distribution $S_D(\underline{r},E)$ is calculated according to eq. (1). In the second step $S_D^{U5,U8}(r,E)$ acts as neutron source and the neutrons fluxes $\phi_2^{U5,U8}$ due to these sources are calculated. All calculations are done in spherical geometry.

4. Neutron flux measurements

In an actual borehole run the composition of the mineral bearing rock (the matrix) is generally unknown. The Uranium concentration is determined from neutron flux measurements done in the borehole. Measurable are thermal and epithermal neutron fluxes ϕ_1^{th} and ϕ_1^{epi} during the irradiation cycle and the total delayed neutron intensity CR during the measuring cycle. These quantities are influenced by the density, water content and neutron absorber concentration of the matrix and in case of water filled borehole by the thickness of the water layer between rock and probe.

The dependence of ϕ_1^{th} and ϕ_1^{epi} from matrix composition and borehole configuration has been determined experimentally. In fig. 1 the dependence of ϕ_1^{th} in Hornblende sand of density 2 g/cm^3 containing 1,7 % water is shown for three different cases: dry borehole and borehole with water layer (wL) of thickness of 4,7 mm and 12,2 mm between neutron source and borehole wall. The composition of Hornblende sand is given in table 3. The macroscopic thermal neutron absorption cross section Σ_a^{th} of the sand used is equivalent to 93 ppm Bor. An evaluation of Σ_a^{th} for different rock types /16/ showed that the B_{nat} equivalent varied between 60 and 90 ppm B assuming a density of 2 g/cm^3. Actually the rock density is higher thus the Hornblende sand used as basic matrix material lies within the range of the B equivalent of actual rocks.

Sands with various compositions were prepared. Different water contents were simulated by adding the respective hydrogen content using Mg-stearate. Li_2CO_3 was added as neutron absorber. Homogeneous mixtures with water content between 1.7 and 10 % and absorber concentrations corresponding to the addition of up to 500 ppm B were prepared. Variations in neutron absorber content in actual rocks will hardly amount up to 500 ppm B. Therefore this case is considered as an extreme upper limit.

In fig. 2 measured ϕ_1^{th}/ϕ_1^{epi} values are plotted for different matrix compositions and different borehole configurations. The values were determined using a ^{252}Cf neutron source. They are used in the evaluation of matrix effects for DFN and PFN. They are valid also for a 14 MeV neutron source. The ratio ϕ_{th}/ϕ_{epi} is only dependent on the slowing down and thermalisation properties of the material surrounding the neutron source. This arises from the fact that an epithermal neutron has forgotten completely from what energy it was started. In case of DFN with a ^{252}Cf neutron source measured neutron flux profiles $\phi_1(r)$ were used for evaluation of matrix effects whereas in case of DFN with 14 MeV and PFN these profiles were calculated.

5. Neutron flux calculations for DFN

Neutron flux calculations were performed using the S_N code DTK /18/ and the KFKINR group cross section set /19/. A dry borehole and water filled boreholes with water layer thickness of 4.7 mm, 12.2 mm and 29 mm between probe and rock were considered. The matrix water content was varied between 0,5 and 20 %. Three additional neutron absorber contents equivalent to 50 ppm, 170 ppm and 500 ppm B were considered. In fig. 1 there are shown also calculated thermal neutron flux profiles ϕ_1^{th}. The calculated profiles using spherical geometry are in good agreement with the experimental results.

Calculations were performed for the two neutron sources ^{252}Cf and 14 MeV neutron generator. The highest neutron energy group in the cross section set KFKINR used for the calculations ranges from 6.5 to 10.5 MeV. To treat the fast fission in U-238 in case of a 14 MeV neutron source

it is assumed that at energies above 1 MeV the neutron energy spectrum is only weakly dependent on the source energy. That means the energy spectrum of a source emitting neutrons with energies between 10,5 and 14 MeV can be approximated by the energy spectrum of a source emitting neutrons between 6,5 and 10,5 MeV. Thus ^{238}U fission rates were determined using calculated neutron flux values in the range below 10,5 MeV and fission cross sections extended to 14 MeV. Simulating the 14 MeV neutron source in the range 6,5 - 10,5 MeV does not affect relative changes in neutron fluxes at low energies due to matrix effects. Fission in U-235 remains also unchanged.

As fission in ^{235}U is mainly induced by thermal neutrons whereas only fast neutrons induce fission in ^{238}U CR(U8) and CR(U5) show a different matrix dependence and are thus discussed separately. In the following values of $CR^* = CR/F(t)$ are given assuming a 1/v detector of thermal sensitivity of 1 cps/nv a source strength of 10^8 n/sec and an ore grade of 1 % U. In case of DFN activation to saturation is assumed thus F(t) = 1 i.e. $CR = CR^*$.

6. Matrix effects for DFN using ^{252}Cf

Calculated delayed fission neutron countrates CR^* are shown in fig. 3 for the case of dry borehole and in fig. 4 for a borehole with 4,7 mm water layer. The contribution of ^{238}U and of thermal and epithermal fission in ^{235}U are separated. In case of unpoisoned matrix and dry borehole the contribution of ^{238}U to the total countrate is less than 10 %. It amounts up to 50 % in case of high absorber and low water content of the matrix. The situation for water filled borehole is similar.

The increase of $CR^*(U8)$ with increasing matrix water content is due to the increased thermalization of the induced fission neutrons in the matrix which overcompensates the decrease in the primary fast neutron flux $\phi_1^S(r,E)$ adjacent to the borehole. $CR^*(U5)$ shows only a slightly increased dependence on matrix water content despite the fact that the thermal neutron flux ϕ_1^{th} depends on matrix water content. The most striking effect is the independence of $CR^*(U5_{epi})$ i.e. the total countrate resulting from fission in ^{235}U due to epithermal neutrons, of the matrix water content.

There are three different effects governing the ^{235}U countrates which partly compensate each other: 1) the inducing low energetic neutron flux profiles become steeper with increasing matrix water content, 2) the intensity of low energetic primary neutrons increases with increasing matrix water content, 3) the conversion of induced fast fission neutrons to slow neutrons is improved. Effect 2) clearly increases CR^* but effect 1) decreases CR^* with increasing matrix water content because of a reduction of the total source intensity $\int_V S_D(r)dr^3$ thus leading to a reduced volume of analysis. Effect 3) causes an increase of $CR^*(U5)$ with increasing matrix water content as is the case with $CR^*(U8)$.

In terms of these effects the behaviour of $CR^*(U5_{th})$ and $CR^*(U5_{epi})$ can be understood as follows: The epithermal primary neutron intensity in and near the borehole increases with increasing matrix water content, but the flux profile in the matrix becomes considerably steeper as is demonstrated in fig. 5 for two different matrix water contents. Effect 3) causes an increase of CR^* with increasing water content as well as effect 2). They are compensated by effect 1). For the behaviour of $CR(U5_{th})$ effect 2) is dominant however damped somewhat by effect 1). The dependence of the thermal neutron flux profile $\phi_1^{th}(r)$ on matrix water content is also shown in fig. 5.

The matrix dependence of the reaction rate profiles $R_f(r)$ causes the volume of analysis to become matrix dependent. In fig. 6 the fraction of delayed neutron intensity coming from a region of radius R is plotted versus R. The borehole configuration only weakly influences the volume of analysis. The influence of matrix water content is large. For 1.7 % water in the matrix 80 % of the delayed neutron intensity is contributed from a sphere of radius of 39 cm i.e. from a volume of 250 l. In case of 10 % water in the matrix the corresponding values are 20 cm and 35 l.

The results given in figs. 3 and 4 are calculated. However thermal and epithermal neutron flux profiles as well as thermal to epithermal flux ratios ϕ^{th}/ϕ^{epi} were determined experimentally for matrix water content between 1.7 and 10 % poisoning of the matrix up to 500 ppm B and different borehole configurations. The experimentally obtained flux profiles can be used to check the calculational results as they make possible a calculation of the fission source distribution $S_D^{U5}(r,E) = \chi(E)R_f^{U5}(r)$. However for arriving at CR^* one calculational step (the conversion of $S_D^{U5}(r,E)$ into ϕ_2^{U5}) is still to be done. As fast fluxes were not systematically measured calculated values $CR^*(U8)$ were used for the determination of the total $CR^*(U)$ the contribution of U-35 to $CR^*(U)$ being dominant. Deviations less than 15 % were found between the calculated CR^+ and those obtained as described above.

7. Concentration determination for DFN using ^{252}Cf

The strong influence of matrix properties on Uranium concentration determination is demonstrated in figs. 3 and 4. If only CR^* would be measured then the uncertainty in C_U could arise in principle to a factor of 200, assuming for instance the range of variation of matrix water content between 1,0 and 10 % and of additional neutron absorber content due to small amounts of Li, B, Cl or rare earth elements up to 500 ppm B_{nat}. Therefore additional quantities have to be measured in order to minimize the influence of matrix properties. The primary neutron flux ϕ_1 is a suitable quantity, measurable during the activation cycle.

A relation between the measurable quantities CR^* and ϕ_1 is required. Several approximations were tried. A correlation of CR^*_{ges} with ϕ_1^{th}/ϕ_1^{epi} seems to be suited. This is shown in fig. 7. The upper line belongs to the case of unpoisoned matrix i.e. without additional neutron absorber additionally. Shown are the cases of poisoned matrices with 50 ppm, 170 ppm and as extreme case poisoning with 500 ppm B_{nat}. The solid lines are belonging to different matrix water content ranging from 1.7 to 10 weight % H_2O. Different borehole conditions i.e. dry borehole, borehole with water layers of thickness of 4.7 mm and 12.2 mm were considered. These are indicated using different symbols.

As is seen from fig. 7 the dependence of CR^* on ϕ_1^{th}/ϕ_1^{epi} is only weakly influenced by water in the borehole. If the thickness of the water layer between probe and borehole wall increases from 0 to 12.2 mm the deviation in CR^* amounts up to ± 12 %. The correlation is independent of matrix water content and is mainly influenced by neutron absorbers possibly being present in the matrix. Admitting the range of neutron poison content between unpoisoned and 170 ppm B_{nat} equivalent

leads to a systematic error in CR^* ($\Delta CR^*/CR^*$) and hence in the Uranium concentration C_U of order of 38 %. This error given as the relative change of the appropriate correlation curves is indicated in fig. 7.

Increasing the water content from 10 % to 20 % and assuming a water layer thickness of up to 12 mm results in an extension of the curves to higher ϕ_1^{th}/ϕ_1^{epi} values as indicated in the figure by the dotted lines. Decreasing the matrix water content below 1.7 % means an extension of the correlation to smaller ϕ_1^{th}/ϕ_1^{epi} values. This is indicated also in fig. 7 for water contents between 0,5 and 1.7 % by the dotted lines.

In fig. 7 there is also shown the extreme case of a water layer of thickness of 29 mm. Increasing the water layer thickness reduces the dependence of ϕ_1^{th}/ϕ_1^{epi} and of CR^* on the matrix water content. The dependence of CR^* on neutron absorber content is increased only slightly. In that case a measurement of CR^* alone would be sufficient for obtaining meaningful results on Uranium concentration.

Trying to decrease the influence of neutron absorber content of the matrix a correlation between the epithermal delayed neutron countrate CR^*_{epi} and ϕ_1^{th}/ϕ_1^{epi} was checked also. CR^*_{epi} depends only weakly on the water content of the matrix. This is shown in fig. 8 for matrix water content in the range between 1.7 and 10 %. CR^*_{epi} shows a somewhat reduced dependence on neutron absorber content of the matrix. Admitting a variation in neutron absorber content between 0 and 170 ppm B_{nat} results in an error in CR^*_{epi} ($\Delta CR^*_{epi}/CR^*_{epi}$) and hence in concentration determination of 25 %. This improvement compared to the case of measurement of total

delayed neutron intensity is outweighted by a reduction of absolute countrate by a factor between 10 and 30 depending on matrix water content and thickness of water layer in the borehole between probe and borehole wall. Measurement of epithermal delayed neutron intensity is therefore only suited for deposits having a high Uranium concentration. As is seen further from fig. 8 the influence of the thickness of water layer is increased compared to the measurement of total delayed neutron intensity.

Fig. 9 shows the uncertainty in CR^* and hence the uncertainty in concentration determination as function of the admitted range of neutron absorber content of the matrix. Curve 1 is valid if the thickness of the water layer between probe and borehole wall is known. Curve 2 is valid if it varies between 0 and 12.2 mm. The figure demonstrates the influence of neutron absorbers possibly being contained in the Uranium bearing matrix. If thermal and epithermal neutron fluxes are measured during the activation cycle the influence of the matrix water content is eliminated.

8. Matrix effects for DFN using a 14 MeV neutron source

For this method the influence of matrix composition and thickness of water layer in the borehole was determined from neutron flux calculations as described previously. The results are similar to those obtained in case of a ^{252}Cf neutron source. However due to the higher source energy the contribution of delayed neutrons from fission in ^{238}U is increased while the primary thermal neutron flux ϕ_1 in and near the borehole is about a factor of 2 less compared to the case of ^{252}Cf thus decreasing the contribution of fission in ^{235}U. Calculated delayed fission neutron countrates CR^* are shown in fig. 10 in case of dry borehole. Given are the different contributions coming from

fission in both Uranium isotopes. In case of unpoisoned matrix fission in U-238 contributes up to 50 % to the total delayed neutron intensity at saturation (F(t)=1). The relative contribution decreases for increasing matrix water content and reaches approximately 37 % in case of 14 % water. In case of a matrix poisoned with 500 ppm B fission in U-238 contributes up to 75 %.

Recently results of laboratory experiments were reported /5/. In these experiments a SiO_2 matrix was used containing NaCl for simulation of the total macroscopic absorption cross section of actually occuring rocks and containing 14 weight % water. In this case the experimentally determined contribution of fast fission in U-238 to the total delayed neutron intensity at saturation was reported to be 35 %. This compares favourably to 37 % as derived from the calculational results as presented in fig. 10.

A comparison of figs. 3 and 10 shows that the dependence of CR^* on matrix composition (water content and poison concentration) is very similar for both cases, showing a slightly decreased dependence on water content. For DFN with 14 MeV neutrons the dependence on poison concentration is reduced almost by a factor of 2.

In fig. 11 CR^* the delayed neutron intensity at saturation is plotted over ϕ_1^{th}/ϕ_1^{epi} for matrix water variations in the range between 1.7 and 10 %. The cases unpoisoned matrix and matrix poisoned with 50 and 500 ppm B_{nat} equivalent are shown. Different borehole configurations were considered. These are dry borehole and boreholes with water layers of thickness of 4.7, 12.2 and 29 mm. The CR^* values are calculated using eq. (1) - (4). They are plotted versus experimentally determined ϕ_1^{th}/ϕ_1^{epi} values. The dependence of CR^* on

ϕ_1^{th}/ϕ_1^{epi} is quite similar to that one using a ^{252}Cf neutron source. It is only weakly influenced by water in the borehole. The correlation is mainly influenced by neutron absorbers possibly being present in the matrix. It is independent of matrix water content. The error in CR^* due to unknown changes in neutron poison concentration decreases with increasing thickness of water layer between probe and borehole wall. Moreover CR^* depends only weakly on matrix water content if the thickness of the water layer is above 12 mm. In fig. 12 the error in CR^* is plotted as function of neutron poison concentration. The values given are valid for a variation of matrix water content between 1.7 and 10 % admitting a variation of the thickness of the water layer between 0 and 12.2 mm.

In case of a 14 MeV neutron source the delayed neutron countrate CR^* contains delayed neutrons from the reaction $^{17}O(np)^{17}N$. Assuming an oxygen content of the matrix of 47 % as is the case in most rocks /17/ the contribution of the ^{17}O to the delayed neutron countrate corresponds approximately to 400 ppm U assuming the same matrix composition. The $^{17}O(np)^{17}N$ reaction requires fast neutrons. Therefore the delayed neutrons from this reaction shows a similar dependence on matrix properties as those from ^{238}U. This means according to fig. 10 that the dependence of CR^*(O-17) on neutron poison concentration is reduced compared to that of CR^*(U).

The correlation between CR^*(O-17) and the thermal to epithermal neutron flux ratio ϕ_1^{th}/ϕ_1^{epi} is measurable in each borehole in those parts containing no Uranium. This correlation reflects the dependence of CR^*(O-17) from the relevant

matrix parameters water content, density, neutron absorber concentration and borehole configuration. Fig. 13 shows the correlation obtained. It is similar to that one for Uranium (fig. 11) but with strongly reduced dependence on neutron absorber content. The difference in CR^*(O-17) due to an additional poisoning of the matrix with 500 ppm B amounts up to ± 25 %. Therefore using the correlation of CR^*(O-17) over ϕ_1^{th}/ϕ_1^{epi} gives only a rough determination of the neutron absorber equivalent of the matrix. For doing this the additional assumptions has to be made that 1) the oxygen content is constant over the whole length of the borehole and that 2) no change in matrix properties occur in the Uranium bearing layer adjacent to the rock formation for which CR^*(O-17) has been measured.

9. Concentration determination in PFN

The measurement of prompt fission neutrons (PFN) as method for Uranium well logging has been suggested by Czubek /9/. A pulsed neutron generator producing 14 MeV neutrons is used as neutron source. After thermalization the source neutrons are showing an exponential time behaviour with die away time constants above 100 µsec. If Uranium is present in the matrix these thermal neutrons induce fission in U-235 thus the epithermal fission neutrons are showing the same die away time behaviour. This offers the possibility of discrimination between thermalized 14 MeV source neutrons and epithermal prompt fission neutrons.

A borehole probe using the PFN method is being developed /10/. The problem of influence of matrix composition on the Uranium concentration determination was recently considered /12,14/. The results obtained so far indicated that the ratio of thermalized source neutrons and epithermal prompt fission neutrons

would be a suitable quantity for elimination of neutron absorber content of the matrix. But the discussion given in /14/ is very specific. Only the influence of neutron absorber was considered. The influence of changes in matrix water content and borehole configuration was not considered.

For a theoretical investigation of the influence of matrix composition on Uranium concentration determination the problem is reduced to the same separate neutron flux calculational steps as in case of DFN. The thermal primary neutron flux $\phi_1^{th}(r)$ calculated for DFN in case of 14 MeV neutron source is used for calculating the fission source distribution $S_p(r,E)$ according to

$$S_p(r,E) = 0{,}0072 \frac{L}{A} C_U \chi(E) \overline{\nu\sigma_f(U5)}^{th} \phi_1^{th}(r) \qquad (7)$$

$S_p(r,E)$ now acts as neutron source and the epithermal neutron flux ϕ_2 is calculated at the position of the 14 MeV neutron source. Using ϕ_2 finally epithermal countrates for a BF_3 detector of total sensitivity of 1 cps/nv were calculated according to

$$CR_{epi} = \int_{E_{Cd}} \varepsilon(E)\phi_2(E)dE \qquad (8)$$

E_{Cd} being the Cf cutoff energy of the Cd shielded neutron detector of sensitivity $\varepsilon(E)$.

10. Matrix effects for PFN using 14 MeV neutrons

In fig. 14 the correlation of the prompt epithermal fission neutron countrate CR_{epi} is plotted versus CR_1 CR_1 being the total countrate of a source monitoring BF_3 detector measured several msec after end of neutron pulse. This signal clearly also contains fission neutrons. But their contribution to the total countrate is negligible. As is seen from fig. 14 the correlation depends on the neutron absorber content of the matrix and on the borehole configuration. This latter effect is due to the only weak influence of the thickness of the wL in borehole on CR_{epi}. The influence of borehole configuration is also observed in DFN with ^{252}Cf if epithermal delayed fission neutrons are detected (see fig. 8). But it is not so pronounced in that case because of the contribution of fission in U-238. The fast fission decreases the dependence of CR on matrix water content. That means it decreases the slope of the CR curves.

Inspection of the data of fig. 14 shows that the ratio CR_{epi}/CR_1 is only weakly dependent on neutron absorber content of the matrix as long as poisoning of the matrix is below 50 ppm and the thickness of the water layer is below 5 mm. In these cases the influence of neutron absorbers can be eliminated. But now CR_{epi}/CR_1 depends on matrix water content and on thickness of the water layer in the borehole as is demonstrated in fig. 15. The influence of neutron absorber increases again with increasing thickness of the water layer but the dependence of CR_{epi}/CR_1 on matrix water content is considerably decreased. This is shown additionally in fig. 15 for a water layer of 12 and 29 mm thickness. Therefore CR_{epi}/CR_1 would be a suitable quantity for Uranium concentration determination if the thickness of water layer is above 10 mm. But in this case the error in C_U

due to unknown neutron absorber concentration is comparable to DFN with Cf. An additional error arises from the remaining dependence of CR_{epi}/CR_1 on the thickness of the water layer in the borehole.

So far PFN was treated as a stationary problem. Actually time dependent neutron fluxes have to be considered. Time dependent neutron flux calculations are reported in /13/. Some special cases were treated. Thermal neutron die away times and time behaviour of the prompt epithermal fission neutrons were calculated for different water content of a SiO_2 matrix. No effects of water filled boreholes and neutron absorber in the matrix were studied. Also no consideration was given to the dependence of prompt epithermal fission neutron intensity CR_{epi} on matrix water content.

Increasing the water content decreases the die away time τ of fission inducing primary thermal neutron flux ϕ_1^{th}. Increasing the neutron absorber content of the matrix further decreases the die away time τ. The prompt epithermal fission neutrons are showing the same time behaviour as the thermal primary neutron flux. According to fig. 14 the PFN countrate CR_{epi} increases with increasing matrix water content and decreases with increasing neutron absorber content.

If the measuring time interval Δt for PFN is several msec the time integrated PFN countrate CR_p given according to

$$CR_p(\Delta t) = \int_{t_1}^{t_1+\Delta t} \phi_2^{epi}(t)\,dt \qquad (9)$$

with t_1 delay time between end of neutron pulse and begin of measurement of prompt fission neutron intensity will show the same dependence on matrix properties as CR_{epi} plotted in fig. 14 and defined according to

$$CR_{epi} = \int_{E_{Cd}} \varepsilon(E)dE \int_{t=0}^{\infty} \phi_2^{epi}(E,t)dt \qquad (10)$$

Decreasing the time width Δt means a change in the dependence of $CR_p(\Delta t)$ on matrix properties. The dependence on matrix water content is increased the dependence on neutron absorber content is decreased. But the overall dependence of CR_p on matrix properties remains similar to that of CR_{epi}.

PFN offers the possibility of an elimination of the influence of neutron absorber concentration. This is done by measuring additionally the thermal neutron die away time τ of the thermalized source neutrons. The dependence of τ on CR_1 is shown in fig. 15. The τ values are partly taken from literature /13/ and are partly calculated using the time moments method as described in /20/. This method was introduced in the transport program Thermos /21/. The other τ values plotted are estimated using the assumption that a water layer of thickness below 15 mm in the borehole only slightly decreases the τ value of the matrix.

According to fig. 16 τ depends mainly on the neutron absorber content of the matrix thus offering the possibility of its determination. Knowing the macroscopic effectiv thermal neutron absorption cross section of the matrix (the Boron equivalent) the evaluation of Uranium concentration is done using fig. 14. Thus the error is reduced to counting statistics and background problems. It depends further on borehole configuration. A variation in the thickness of water layer in the range between 0 - 12 mm produces a systematic error in C_U of 25 % if the neutron absorber content is below 200 ppm B.

11. Discussion of DFN and PFN

Compared with DFN PFN shows a stronger dependence of the fission neutron countrate on neutron absorber concentration and on borehole configuration. If a die away log is taken the influence of the first on the determination of Uranium concentration is eliminated. But the influence of the borehole configuration remains. If the thickness of the water layer in the borehole varies between 5 and 12 mm the error in C_U is of order of 25 %. If no die away log is taken the systematic error amounts up to 40 % admitting a variation in poison concentration of 50 ppm B and assuming the same variation in the thickness of the water layer. These errors have to be compared with the appropriate errors for DFN with ^{252}Cf of 30 % and DFN with 14 MeV neutrons of 20 %. Therefore from the reason of a minimization of matrix effects PFN gives no advantage compared with DFN.

Applying PFN means use of a relatively complicate measuring technique because of the performance of time dependent measurements. It moreover means problems connected with the long time operation of pulsed neutron generators. According to Bivens et al. /10/ the life time of encapsulated neutron tubes is expected to be a total of 10^7 pulses or about 28 hours at 100 pulses/second.

The advantage of PFN is the high sensitivity and the high logging speed. According to table 2 minimum detectable Uranium concentrations are in the range below 30 ppm U depending on source intensity available and type of deposit. Ore grades of 100 ppm U are detectable with a statistical accuracy of 10 %.

The determination of Uranium concentration using DFN with 14 MeV neutrons is influenced by neutron absorbers possibly being present in the matrix. The other matrix effects can be eliminated (matrix water content) or can be made small (thickness of water layer between probe and rock) by measuring additionally the thermal and epithermal neutron fluxes ϕ^{th} and ϕ^{epi} during the irradiation cycle.

DFN with 14 MeV neutrons is influenced by the reaction $^{17}O(np)^{17}N$ having a threshold at 7.93 MeV and producing delayed neutrons with energies up to 1 MeV. A delayed neutron log of O-17 does not improve the accuracy of results of analysis because of the weak influence of neutron absorber content.

The minimum detectable Uranium concentration C_U^{min} is relatively high because of contribution of delayed neutrons from O-17. These contribute with an equivalent of order of 400 ppm U. Assuming a 2 σ criterion C_U^{min} is about 80 ppm U. The statistical error is 40 % for ore grades of 100 ppm U. Thus in case of low concentration of U DFN with 14 MeV neutrons is inferior to the other methods. The method is advantageously applied in case of Uranium concentrations above 500 ppm U.

DFN with ^{252}Cf is the most simple method. Variations in neutron absorber content of the matrix are influencing the Uranium determination. No possibility exists leading to an elimination of this source of error. The other matrix effects can be eliminated (matrix water content) or can be made small (thickness of water layer) as is the case with DFN with 14 MeV neutrons. DFN with ^{252}Cf offers attractive features for application in Uranium borehole probe. For practical application the most

advantageous arrangement uses a layer of moderating material of thickness above 20 mm around the neutron source. In that case no measurement of thermal and epithermal neutron fluxes during the activation cycle is needed. According to table 2 the probe could be operated continuously. The statistical accuracy obtainable would be approximately 16 % for ore grades of 100 ppm U.

References

/1/ R.D. Nininger
Uranium resources - are they adequate?
Nucl. Technology Vol. 30 224 (1976)

/2/ J.A. Patterson
Uranium supply developments.
Summary report fuel cycle conf.
21 - 24 March 1976, Phoenix Arizona

/3/ P.F. Schutt, J.S. Hobbs
U_3O_3 Supply in technological and commercial transition
Trans.Am.Nucl.Soc. Vol. 21 241 1975

/4/ W. Givens et al.
Uranium assay logging using a pulsed 14 MeV neutron source and detection of delayed fission neutrons
Geophysics Vol. 41 No. 3 468 (1976)

/5/ R.C. Smith, R.G. Rodriguez
Laboratory characterization of pulsed neutron borehole logging for assaying Uranium.
Trans.Am.Nucl.Soc. 23 193 (1976)

/6/ Cf-252 Progress No. 12 31 (1972)

/7/ D.K. Steinmann et al.
^{252}Cf based borehole logging system for in situ assaying of Uranium Ore
IAEA-SM-208/43 Vienna (1976)

/8/ Uranium borehole logging using ^{252}Cf.
Cf-252 Progress No. 20 25 (1976)

/9/ J.A. Czubek
Pulsed neutron method for Uranium well logging
Geophysics Vol. 37 No. 1 160 (1972)

/10/ H.M. Bivens et al.
Pulsed Neutron Uranium borehole logging with epithermal neutron dieaway.
IAEA-SM-208/48 Vienna 29 March - 2 April (1976)

/11/ M.R. Wormald, C.R. Clayton
Some factors affecting accuracy in the direct determination of Uranium by delayed neutron borehole logging
IAEA-SM/208-35 Vienna 29 March - 2 April (1976)

/12/ D.H. Jensen
Prompt fission neutron assay of Uranium boreholes
Trans.Am.Nucl.Soc. 24 114 (1976)

/13/ J.H. Renken
Prediction of time dependent neutron fluxes encountered in pulsed neutron Uranium logging experiments
Nucl. Technology Vol. 31 133 (1976)

/14/ J.H. Renken
Minimization of neutron absorber effects in pulsed neutron Uranium logging
Trans.Am.Nucl.Soc. 24 119 (1976)

/15/ G. Schulze, H. Würz
Mineral exploration in unknown geological formations using (nγ) borehole probes
Symp. on Utilization of Cf-252, Paris, April 26-28 (1976)

/16/ G.R. Keepin
Physics of nuclear kinetics
Addison Wesley Publishing (1967)

/17/ K.H. Wedepohl
Handbook of Geochemistry
Springer Verlag Berlin , Heidelberg, New York (1969)

/18/ C. Günther, W. Kinnebrock
Das eindimensionale Transportprogramm DTK
KFK 1381 (1971)

/19/ E. Kiefhaber
The KFKINR Set of group constants
KFK 1572 (1972)

/20/ A.E. Profio et al.
Measurements and calculations of the slowing down and migration time
IAEA Conf. Pulsed neutron research Vol. I 123 (1965)

/21/ H. Honeck
Thermos Code for reactor lattice calculation
BNL 5826 (1961)

Table 1 a Yield of delayed neutrons from neutron induced fission of ^{235}U

Group	half life sec	decay constant λ_i sec^{-1}	relative yield a_i
1	54,51	0,0127	0,038
2	21,84	0,0317	0,213
3	6,0	0,116	0,188
4	2,23	0,3107	0,407
5	0,496	1,39	0,128
6	0,179	3,87	0,026

total delayed fraction β = 0,0065

Table 1 b Yield of delayed neutrons from fast neutron induced fission of ^{238}U

Group	half life sec	decay constant sec^{-1}	relative yield a_i
1	52,38	0,013	0,013
2	21,58	0,032	0,137
3	5,0	0,138	0,162
4	1,93	0,359	0,388
5	0,493	1,405	0,225
6	0,172	4,03	0,075

total delayed fraction β = 0,0148

Table 2 Minimum detectable Uranium concentration using prompt or delayed fission neutrons

method	ref.	sensitivity (cps/ppm U) neutron source 10^8 n/sec	mode of operation	minimum detectable concentration (ppm U)	statistical accuracy (%) for 100 ppm U
DFN with ^{252}Cf	7	$(1,5\text{-}10)\,10^{-3}$ (1)	continuous v=1,5m/min	20 (2)	< 16
DFN with 14 MeV	5	$(1,5\text{-}7)\,10^{-3}$ (1)	continuous v<2,5m/min	80 (3)	< 10 % if C_U > 500 ppm
PFN	10	$(1,0\text{-}3,0)\,10^{-2}$	continuous v=2,5m/min	< 20 (4)	10

(1) values are at saturation

(2) value is valid for neutron source strength of $5 \cdot 10^8$ n/sec

(3) The contribution of delayed neutrons from $^{17}O(np)^{17}N$ is equivalent to approximately 400 ppm U. This deteriorates the minimum detectable Uranium concentration

(4) a neutron source strength of $5 \cdot 10^8$ n/sec is assumed

Table 3 Chemical composition of Hornblende sand, density 2 g/cm^3

element	% weight	number density atoms/cm^3 x 10^{-24}	σ_{ao}^{th} (barn)
H	0,19	$2,28 \cdot 10^{-3}$	0,32
C	0,17	$1,7 \cdot 10^{-4}$	0,004
O	48,3	$3,65 \cdot 10^{-2}$	--
Mg	4,1	$2,0 \cdot 10^{-3}$	0,069
Al	6,5	$2,9 \cdot 10^{-3}$	0,241
Si	31,4	$1,35 \cdot 10^{-2}$	0,16
Ca	4,56	$1,76 \cdot 10^{-3}$	0,44
Fe	3,96	$8,6 \cdot 10^{-4}$	2,62
W	0,89	$5,85 \cdot 10^{-5}$	19,2
$\Sigma_{a,total}^{th} = 6,91 \cdot 10^{-3}$ (cm^{-1})			

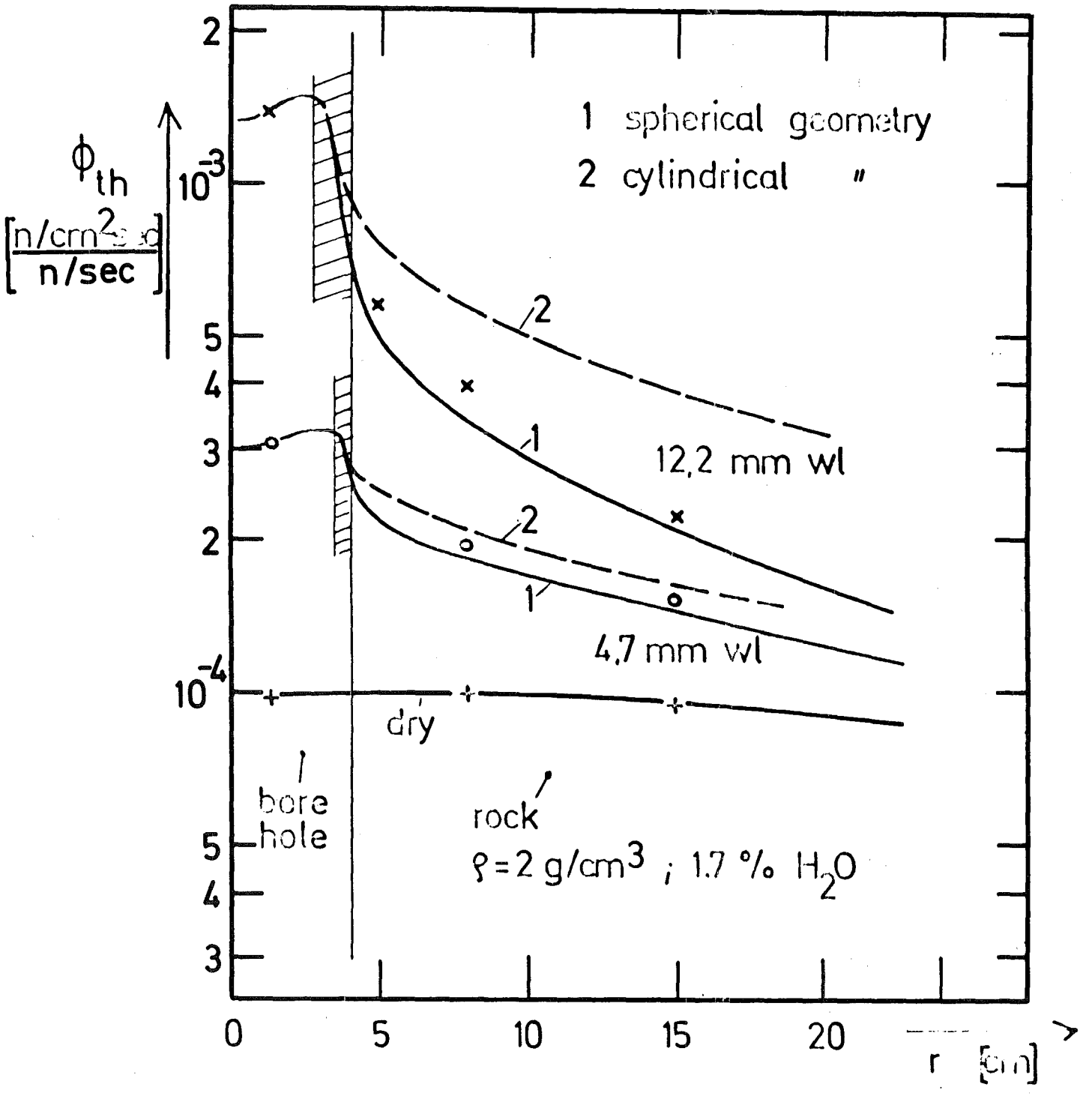

Fig. 1 Measured and calculated thermal neutron fluxes for dry borehole and for borehole with water layer of 4.7 mm and 12.2 mm thickness

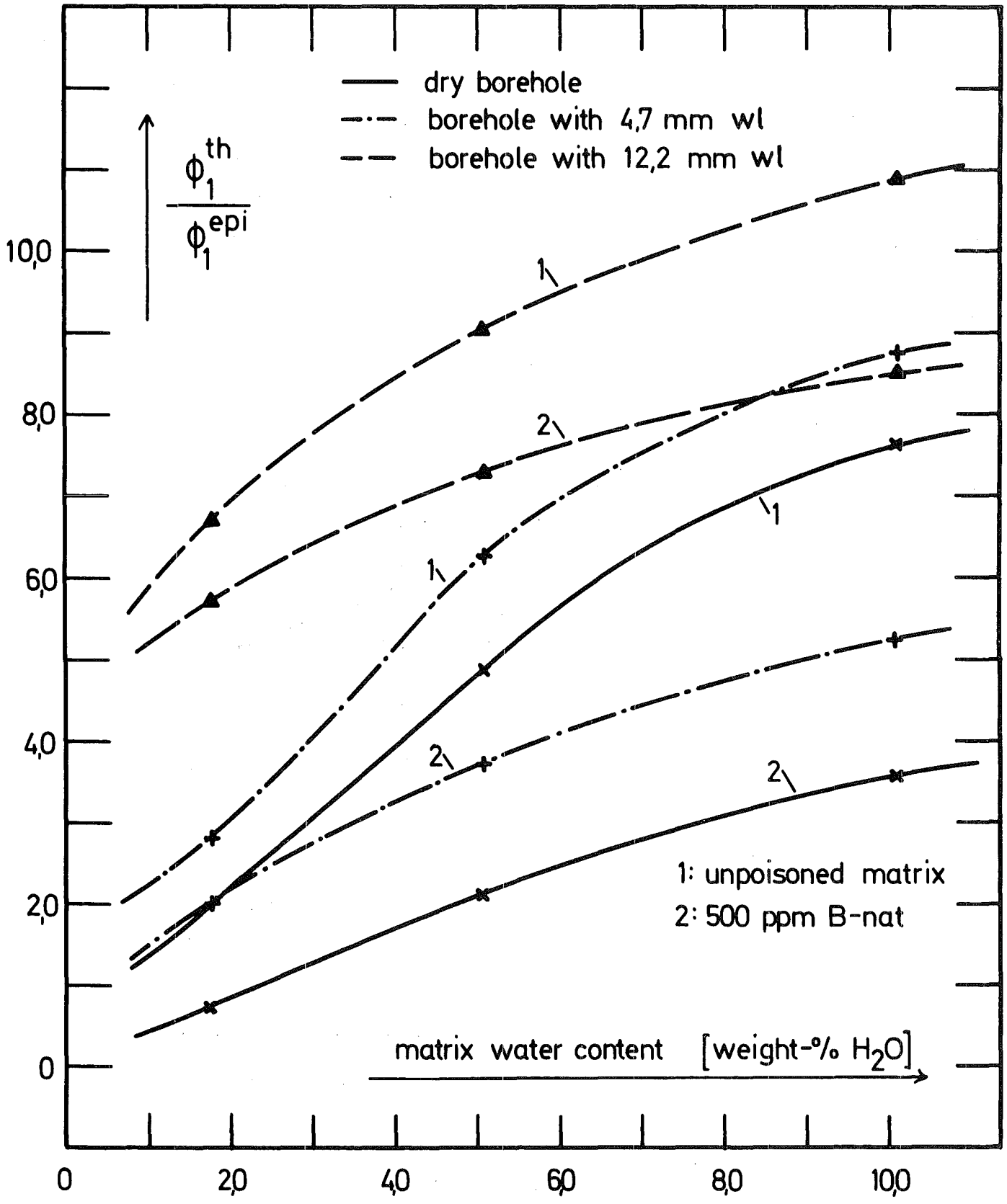

Fig. 2 Measured thermal to epithermal neutron flux ratios for different matrix compositions and different borehole configurations

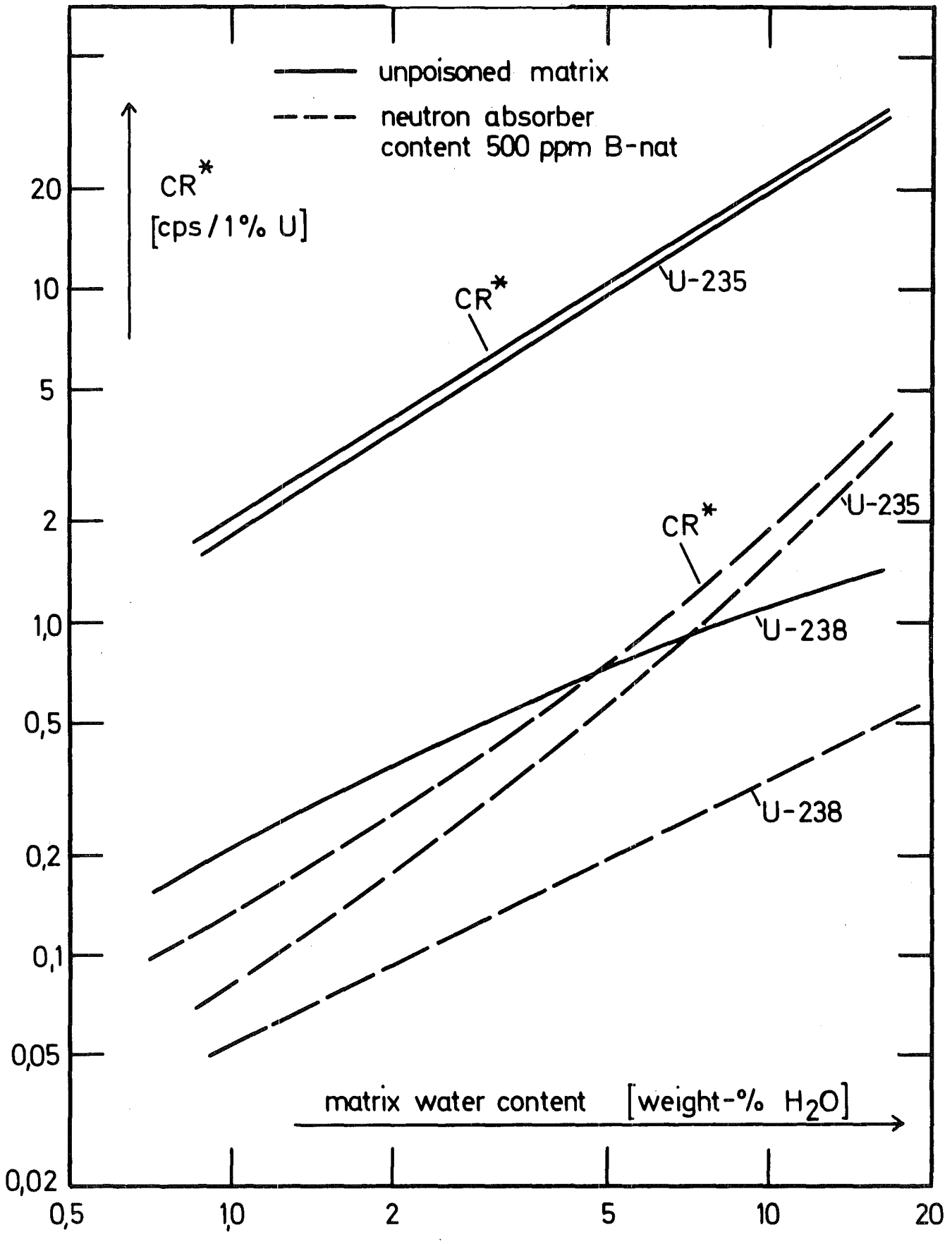

Fig. 3 Calculated delayed fission neutron countrates CR^* for different matrix compositions in case of dry borehole. The values given are valid for a matrix of density 2 g/cm^3 containing 1 % U. The ^{252}Cf neutron source used for activation emits 10^8 n/sec

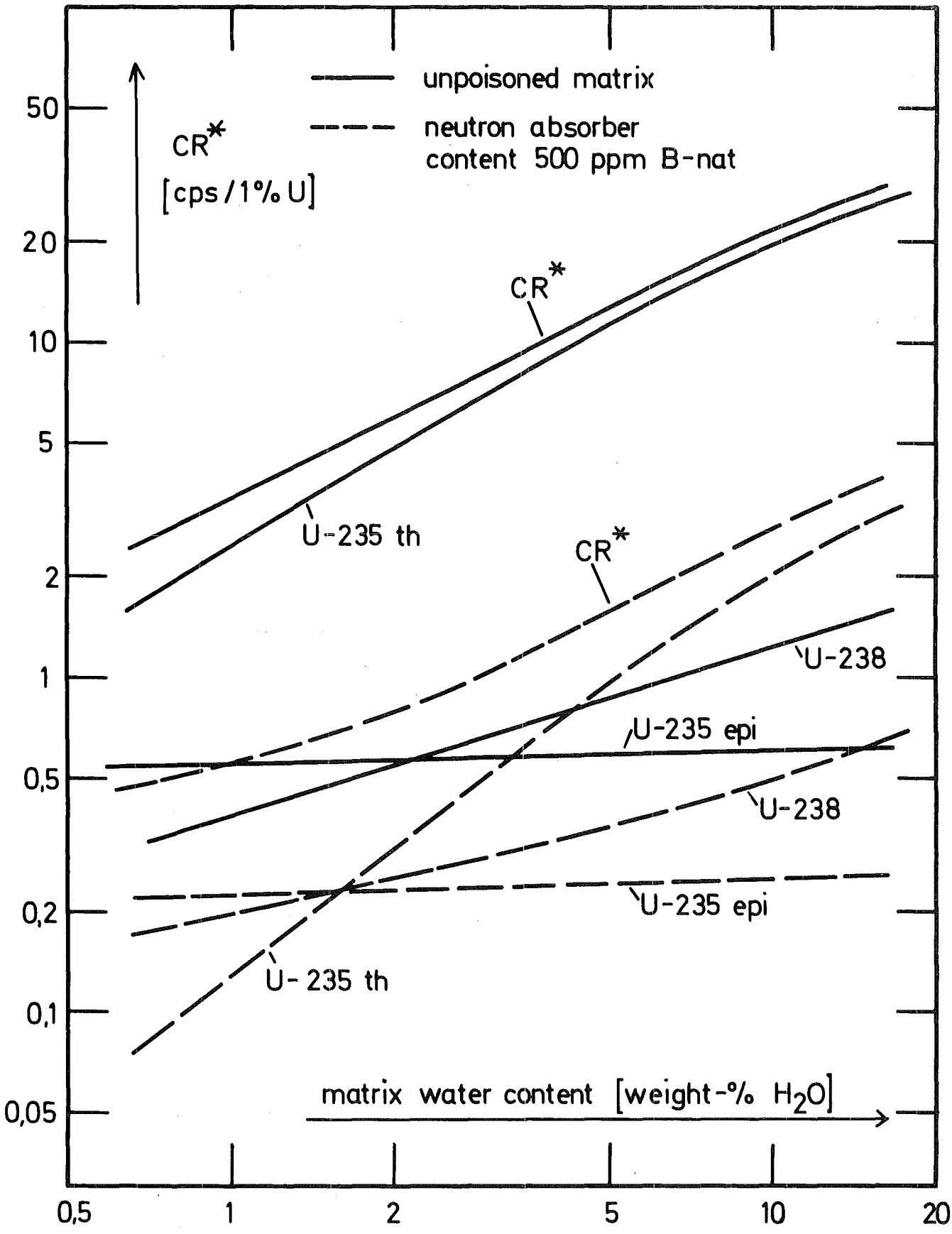

Fig. 4 Calculated delayed fission neutron countrates CR^* in case of borehole with water layer of thickness of 4.7 mm. The matrix contains 1 % U, the ^{252}Cf neutron source emits 10^8 n/sec

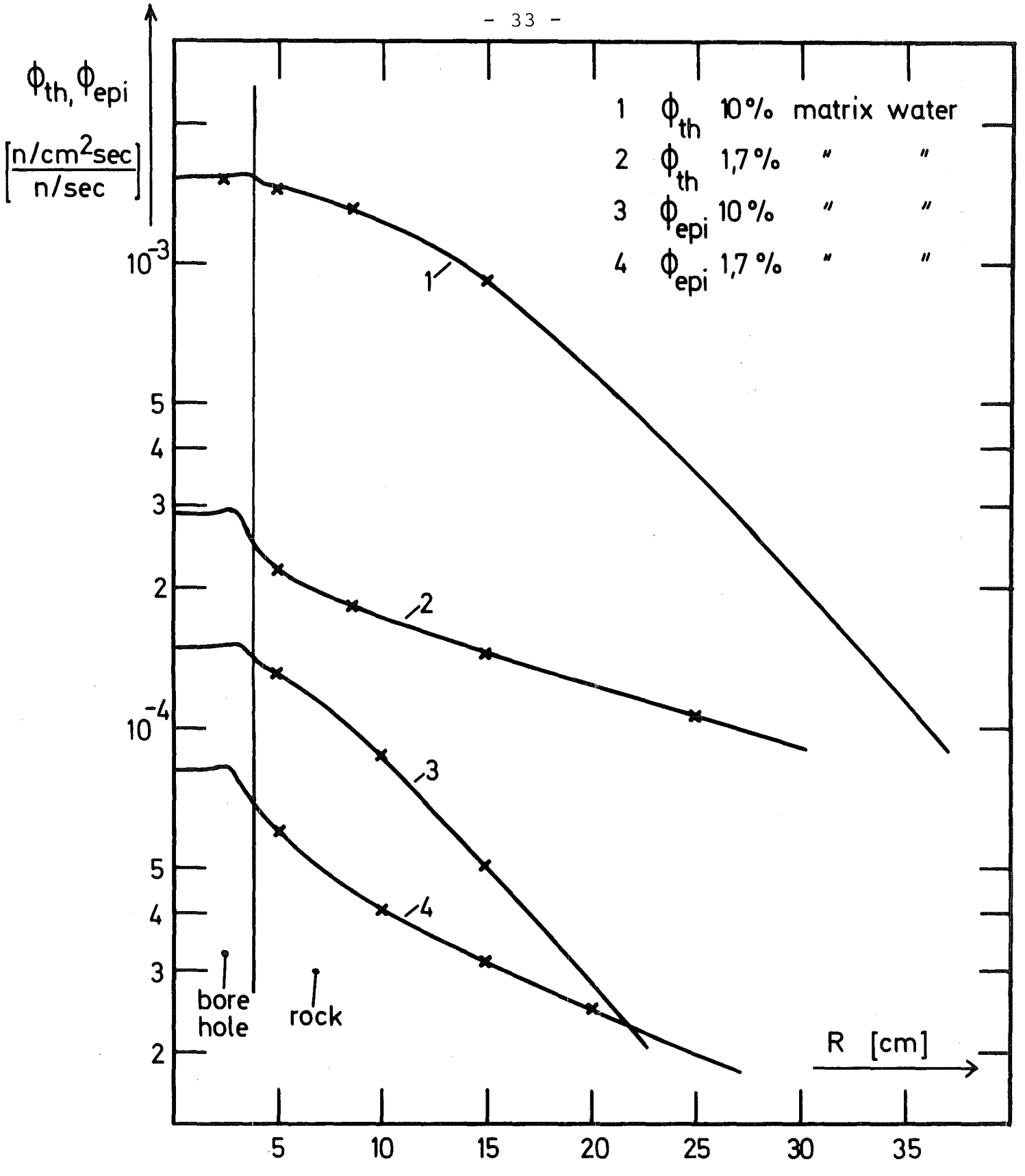

Fig. 5 Measured thermal and epithermal neutron flux profiles for the two matrix water contents 1,7 % and 10 % weight in case of borehole with water layer of 4,7 mm.

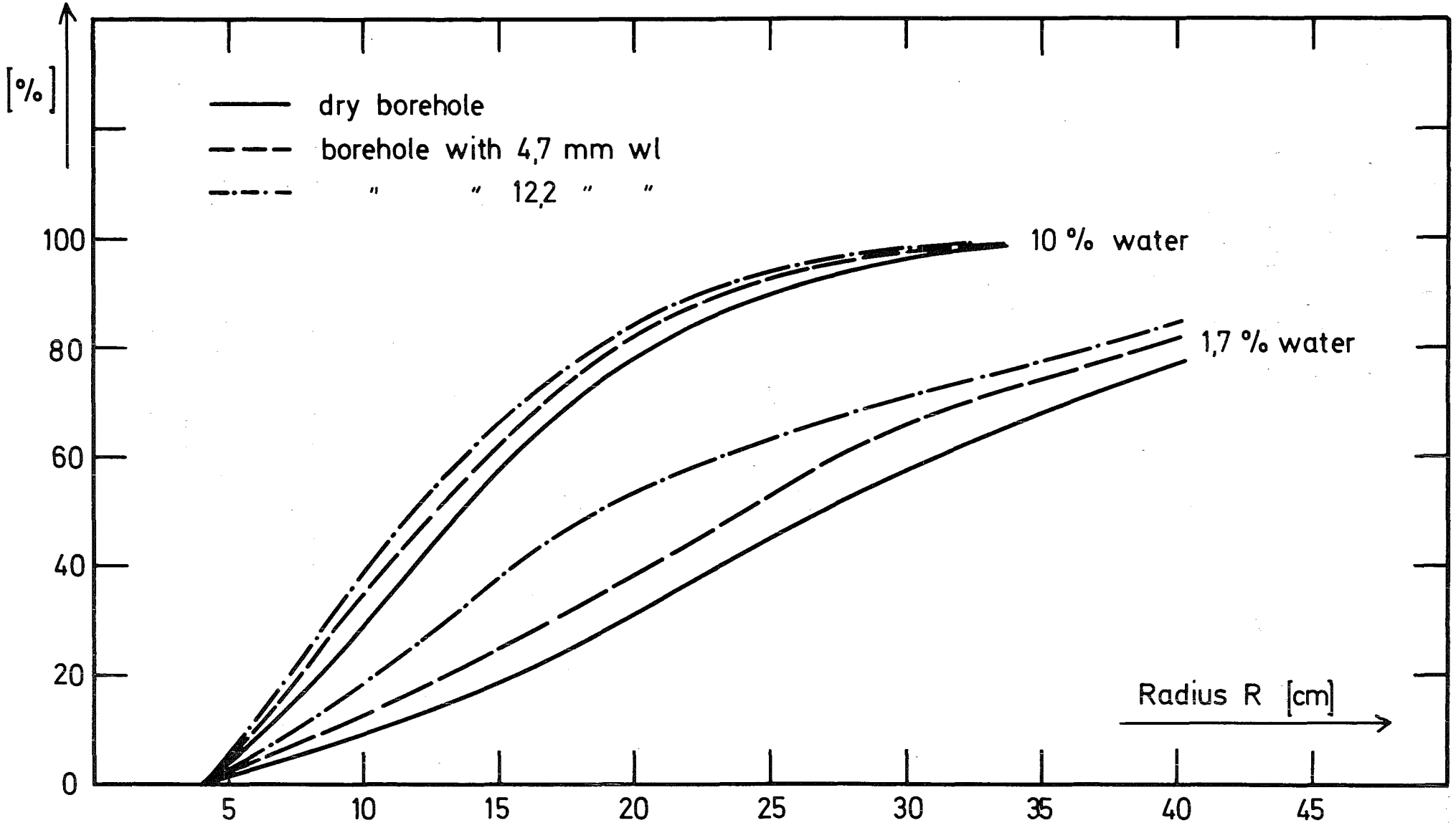

Fig. 6 Volume of analysis for different matrix compositions and different borehole configurations

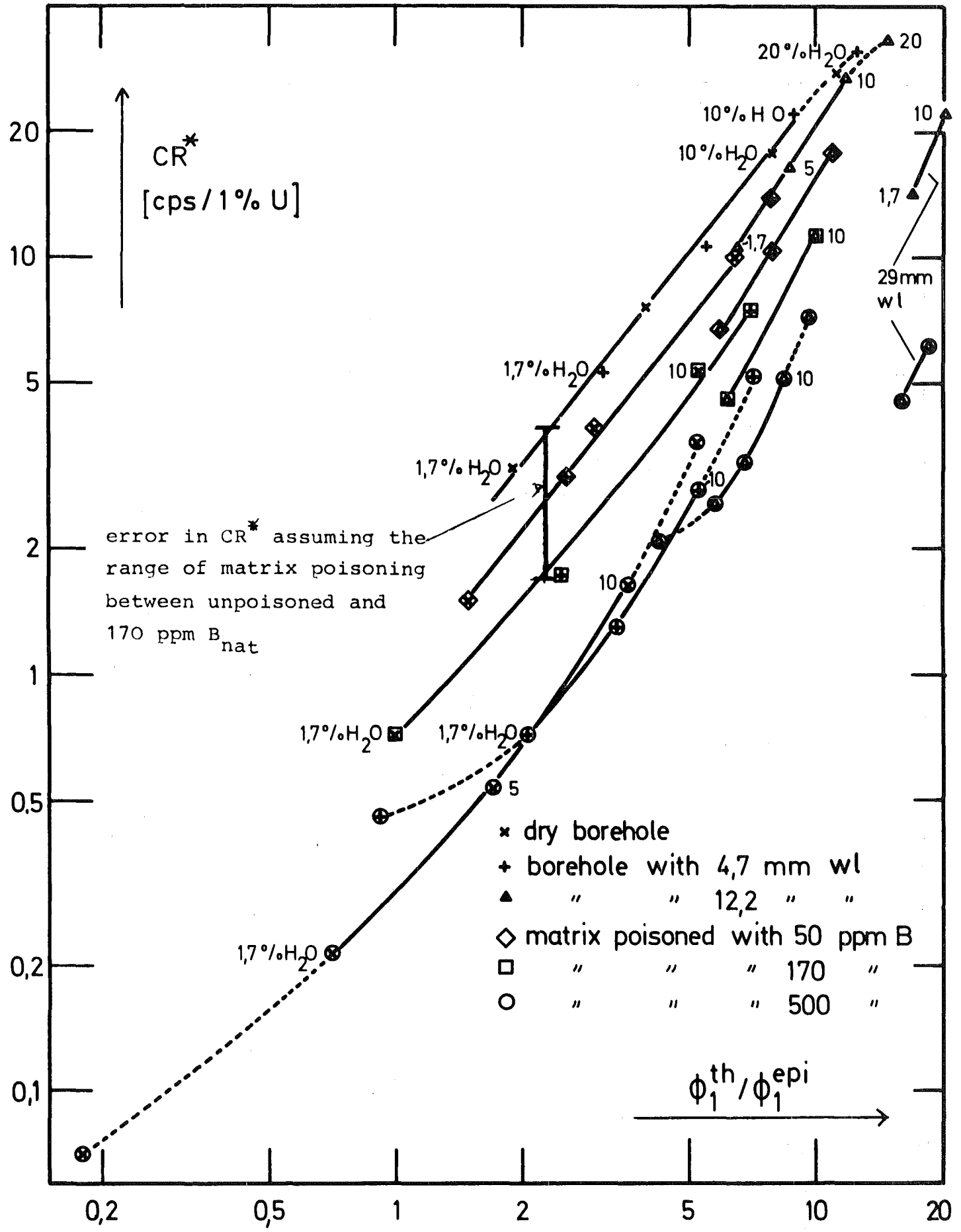

Fig. 7 Total delayed fission neutron countrate CR* versus ratio of thermal to epithermal primary neutron flux as function of matrix composition and borehole configuration. The matrix contains 1 % U, the ^{252}Cf neutron source emits 10^8 n/sec

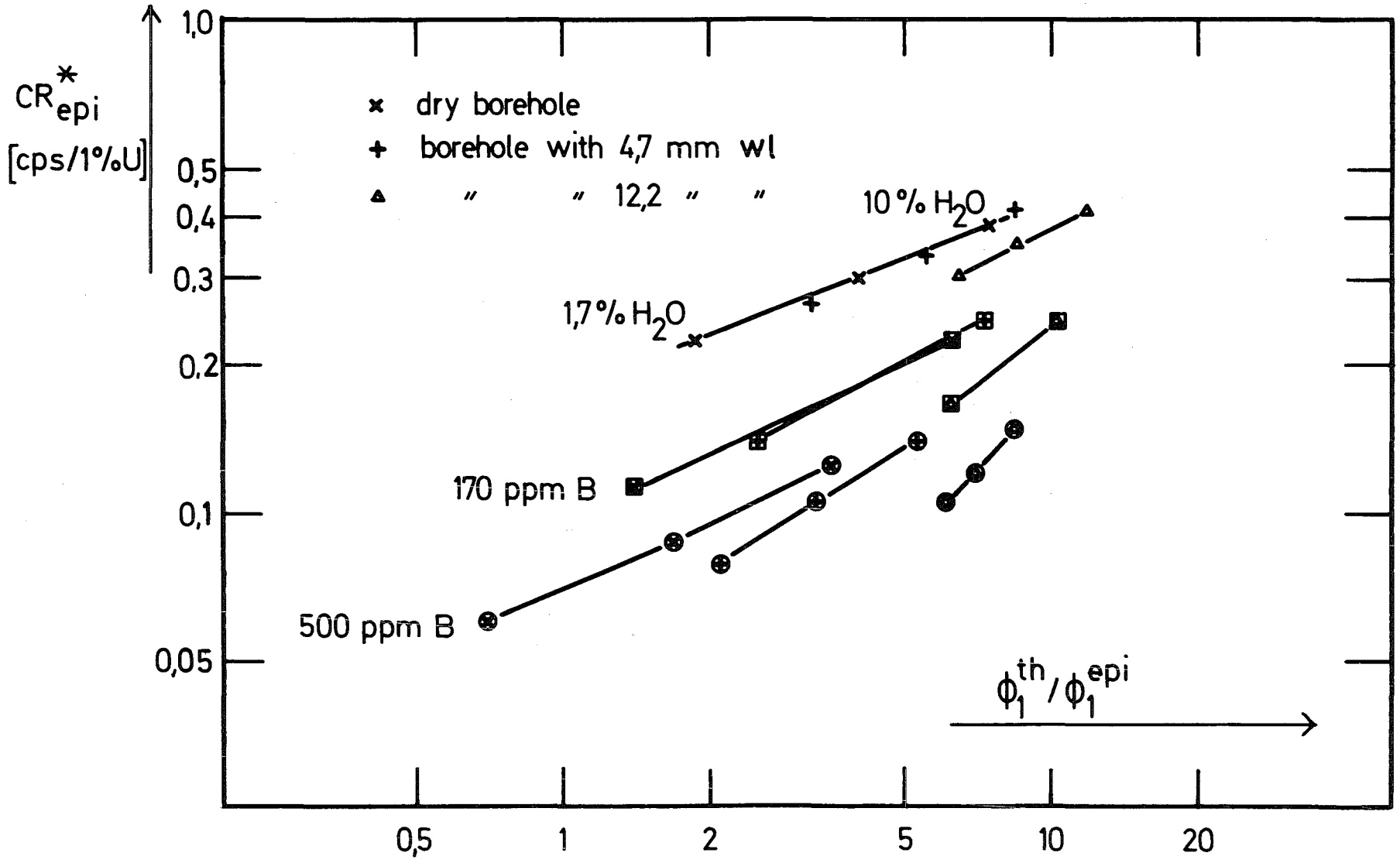

Fig. 8 Epithermal delayed fission neutron countrate CR^*_{epi} versus ratio of thermal to epithermal neutron flux for different matrix compositions and borehole configurations.

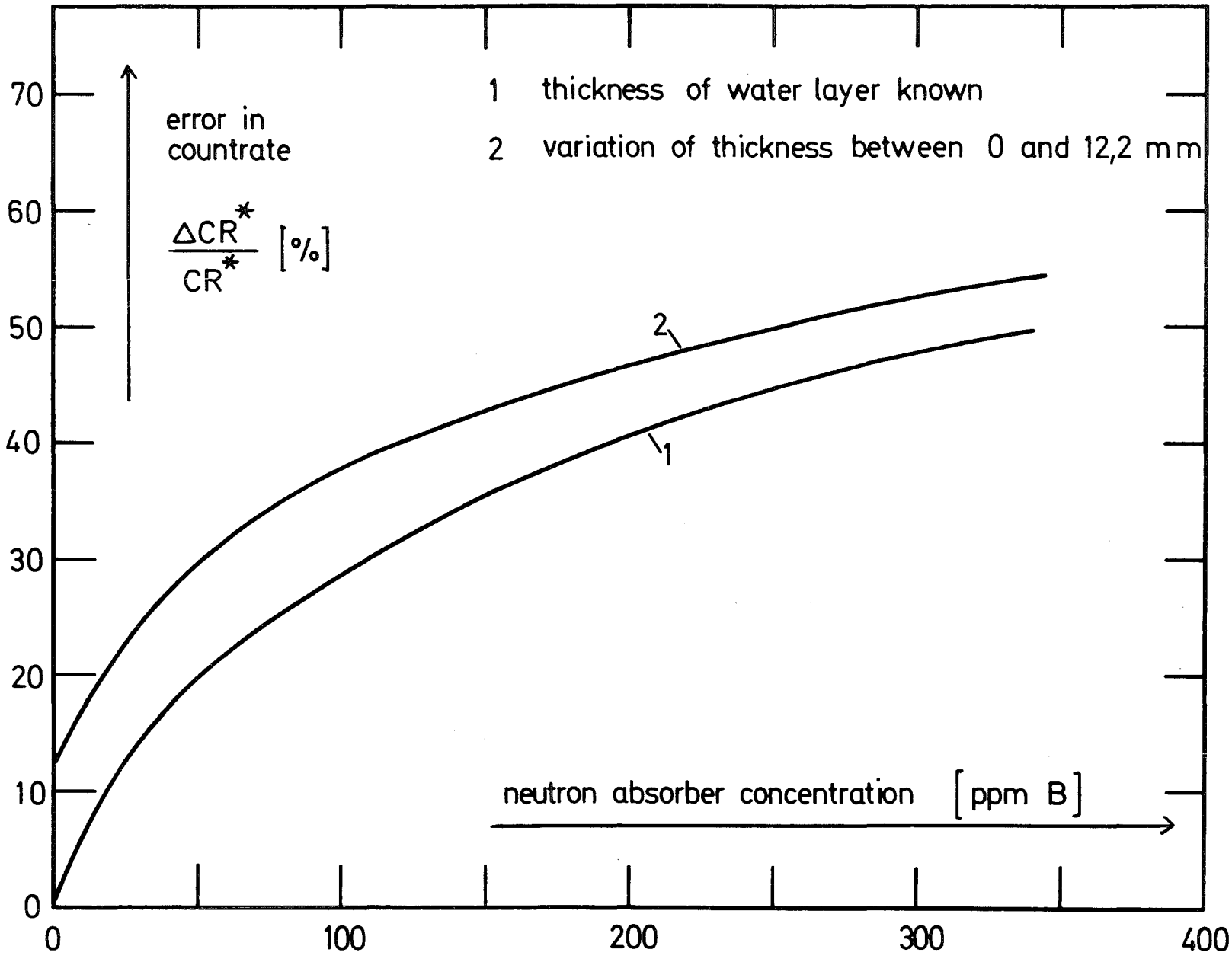

Fig. 9 Systematic error in DFN countrate due to variations in neutron absorber content of the matrix and unknown borehole configuration

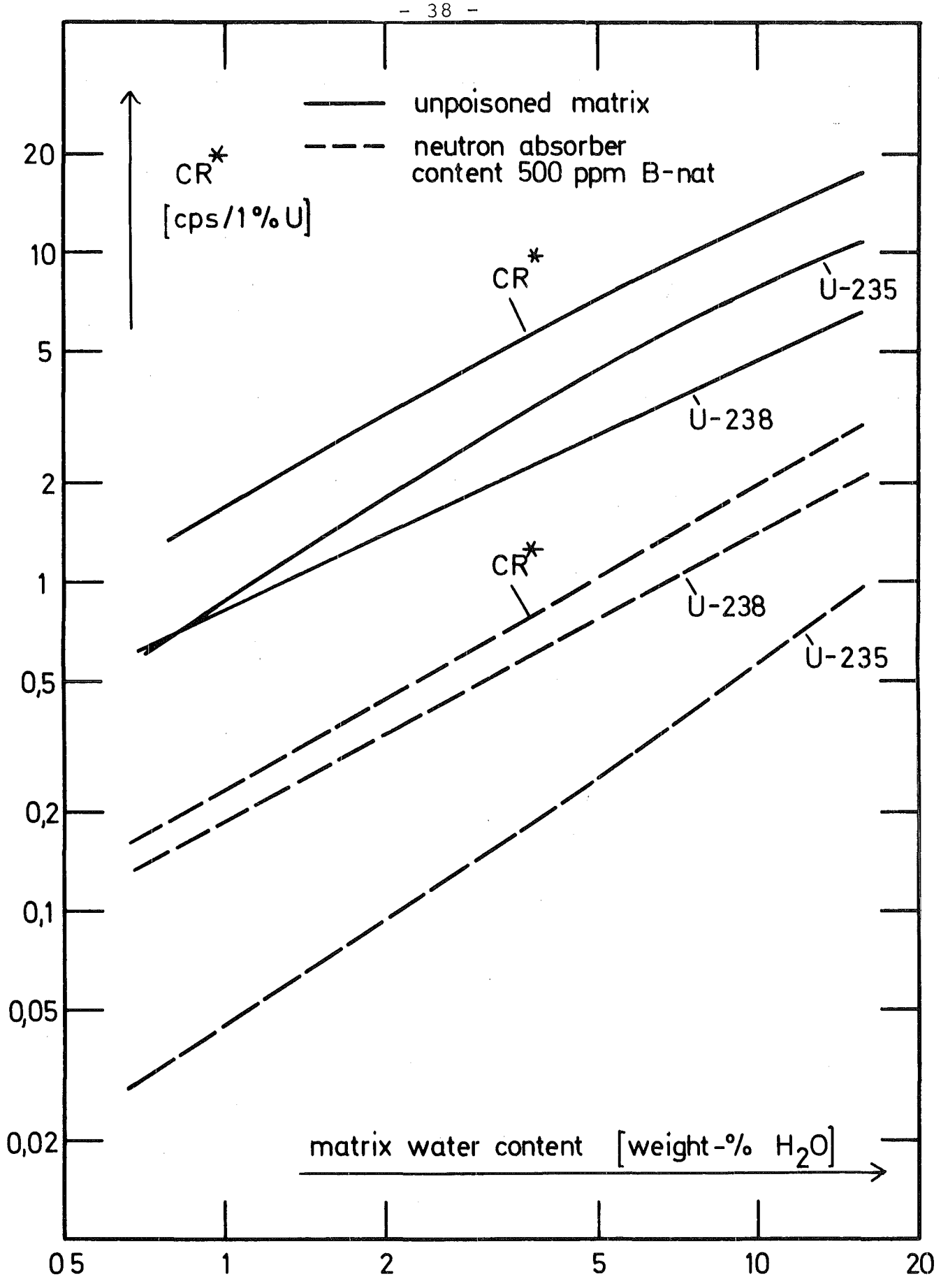

Fig. 10 Calculated delayed fission neutron countrates CR^* in case of borehole with water layer of thickness of 4,7 mm. The matrix contains 1 % U, the 14 MeV neutron source emits 10^8 n/sec

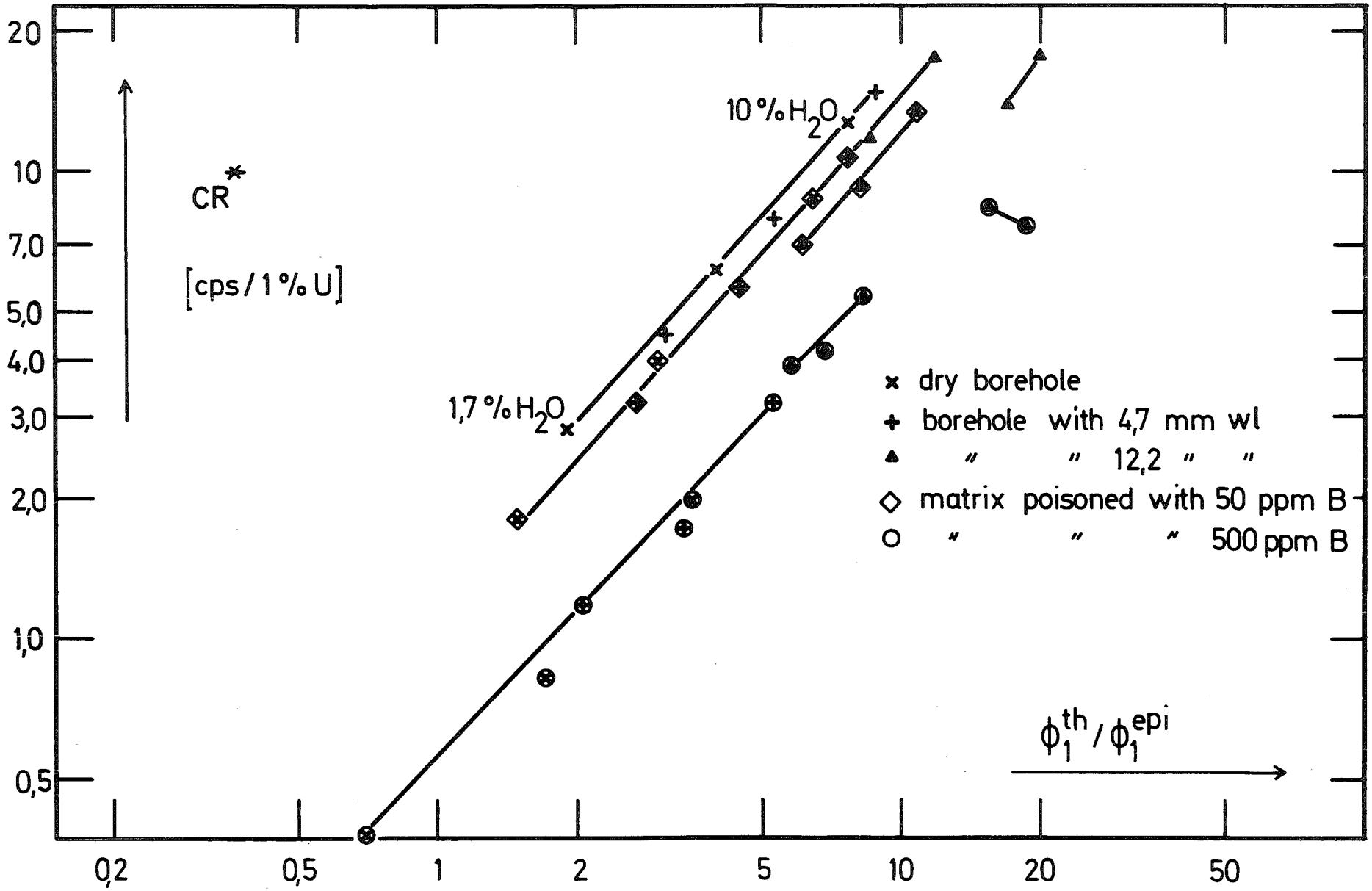

Fig. 11 Total delayed fission neutron countrate CR^* versus ϕ^{th}/ϕ_{epi} as function of matrix composition and borehole configuration. The matrix contains 1 % U. The 14 MeV neutron source emits 10^8 n/sec.

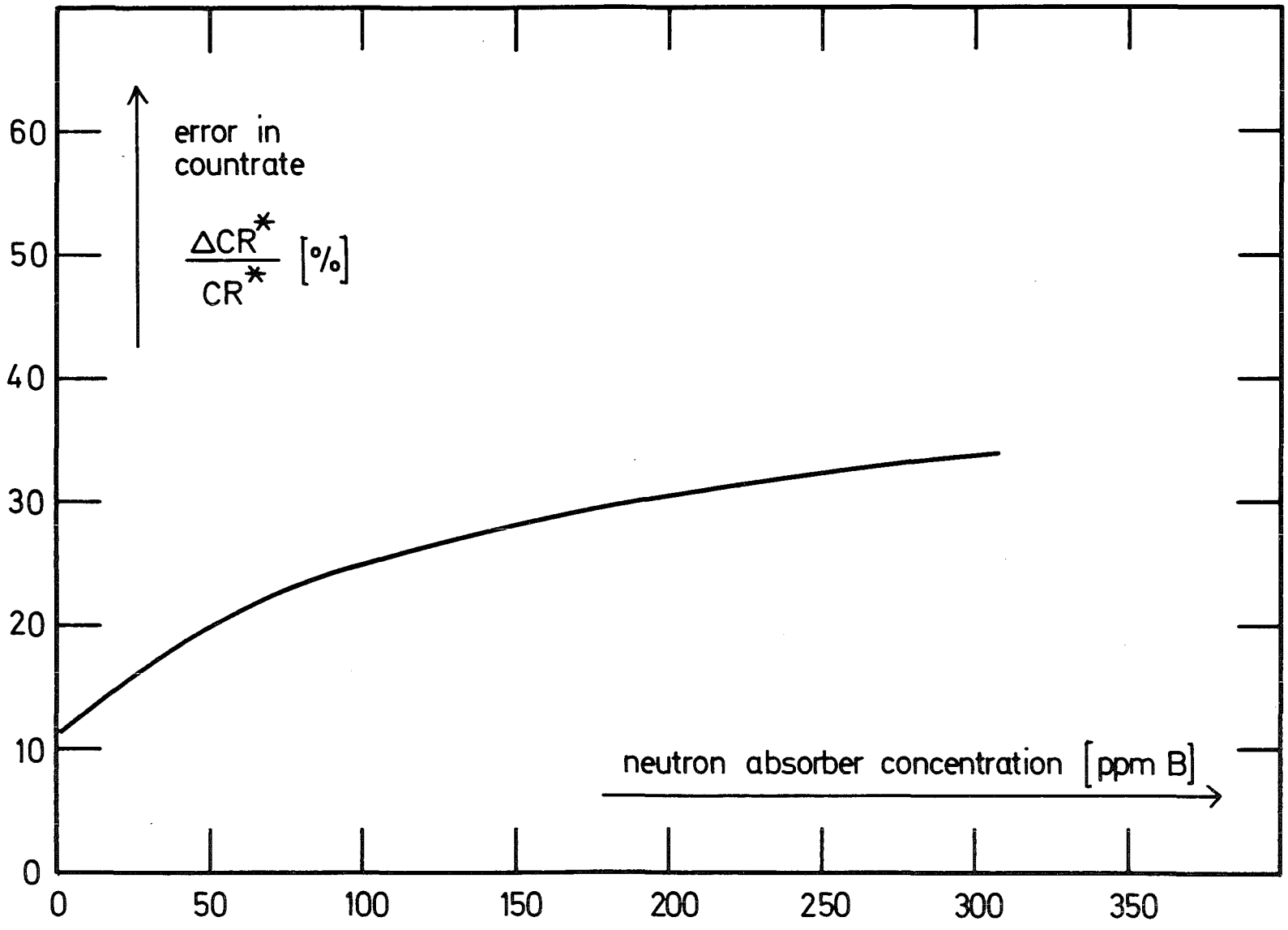

Fig. 12 Systematic error in DFN countrate due to variations in neutron absorber content of the matrix and unknown borehole configuration using a 14 MeV neutron source

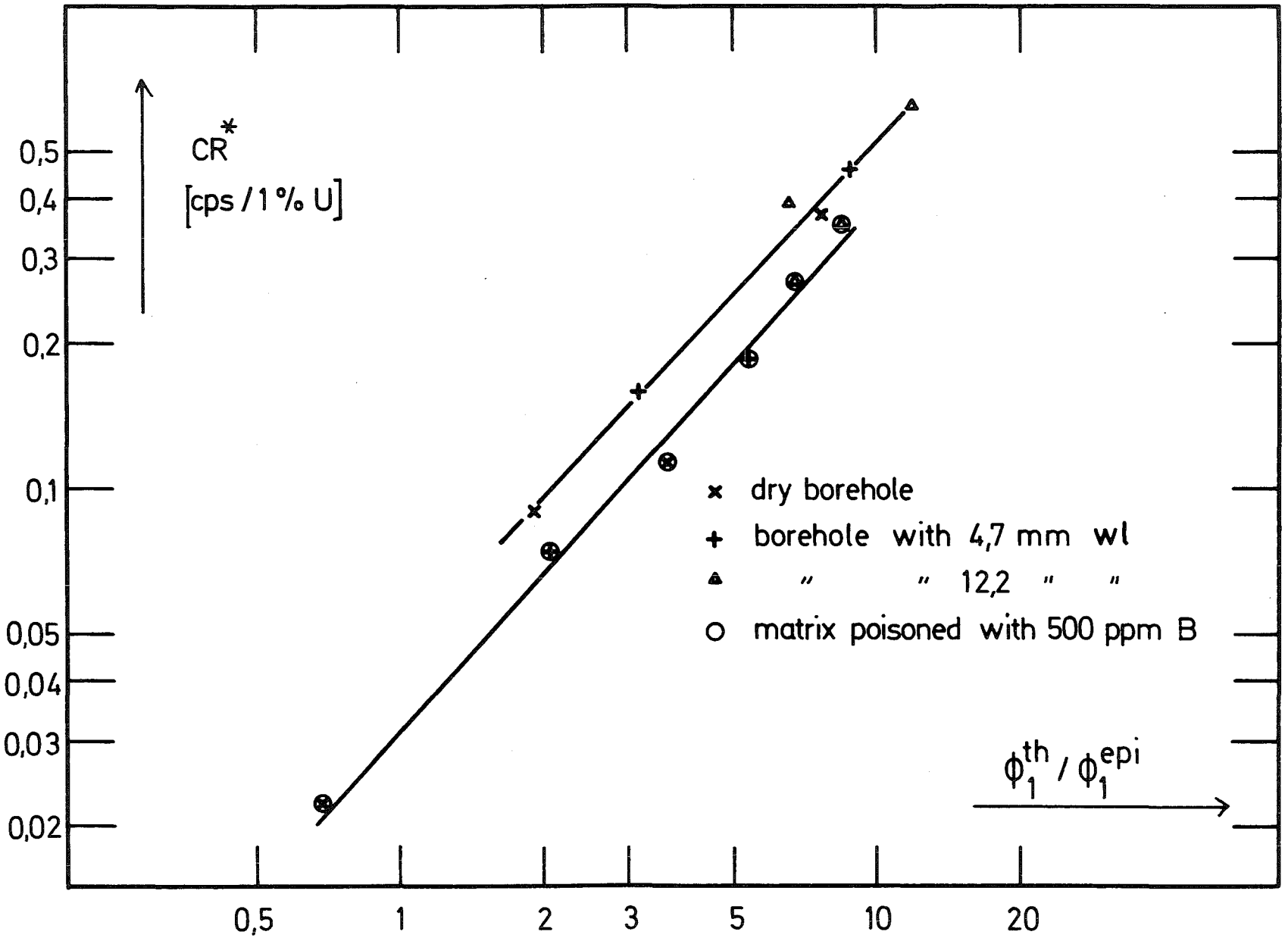

Fig. 13 Total delayed neutron countrate CR^* due to $^{17}O(np)^{17}N$ versus ϕ^{th}/ϕ^{epi} as function of matrix composition and borehole configuration

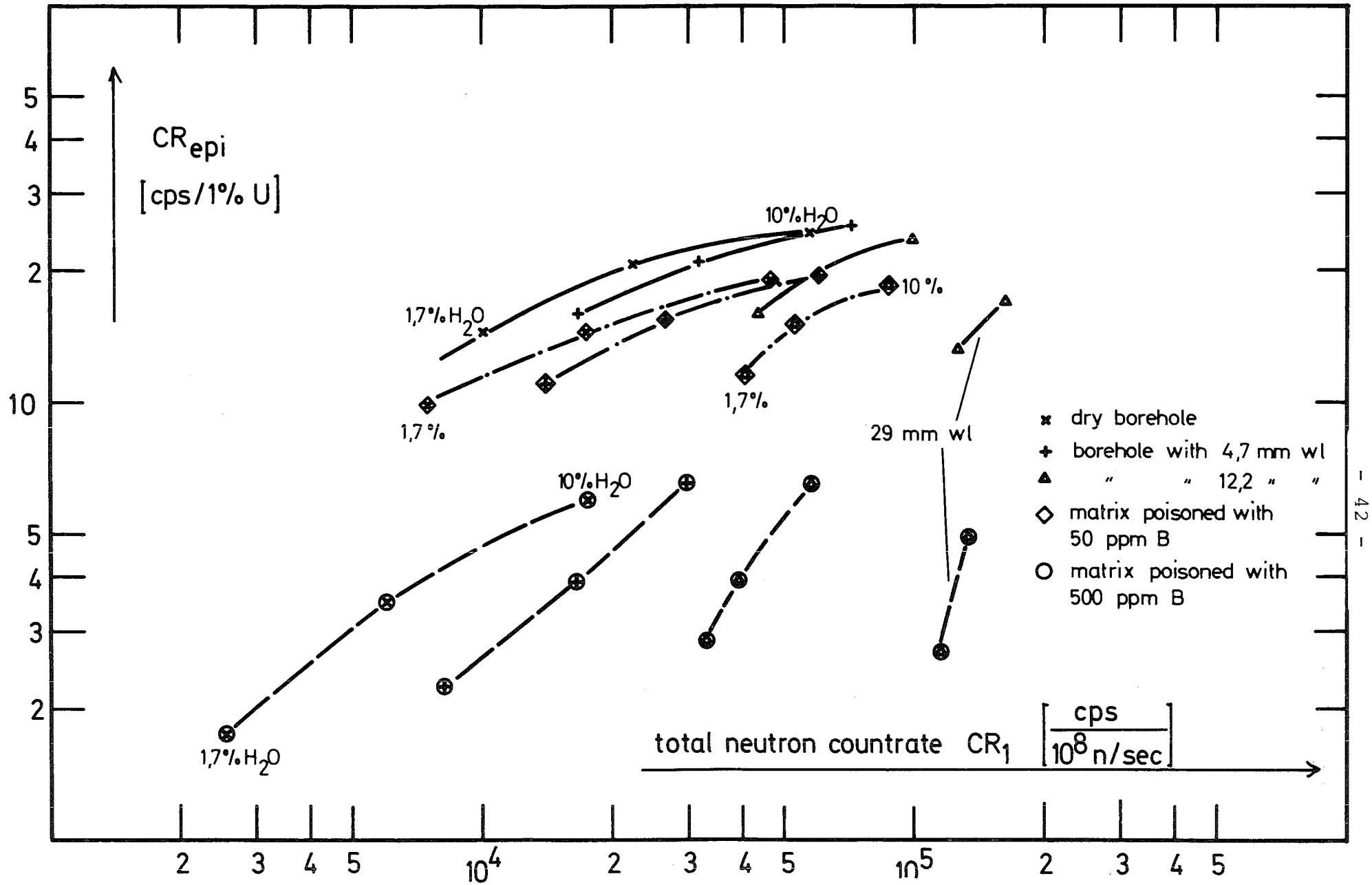

Fig. 14 Epithermal prompt fission neutron countrate CR versus total neutron countrate as function of matrix composition and borehole configuration

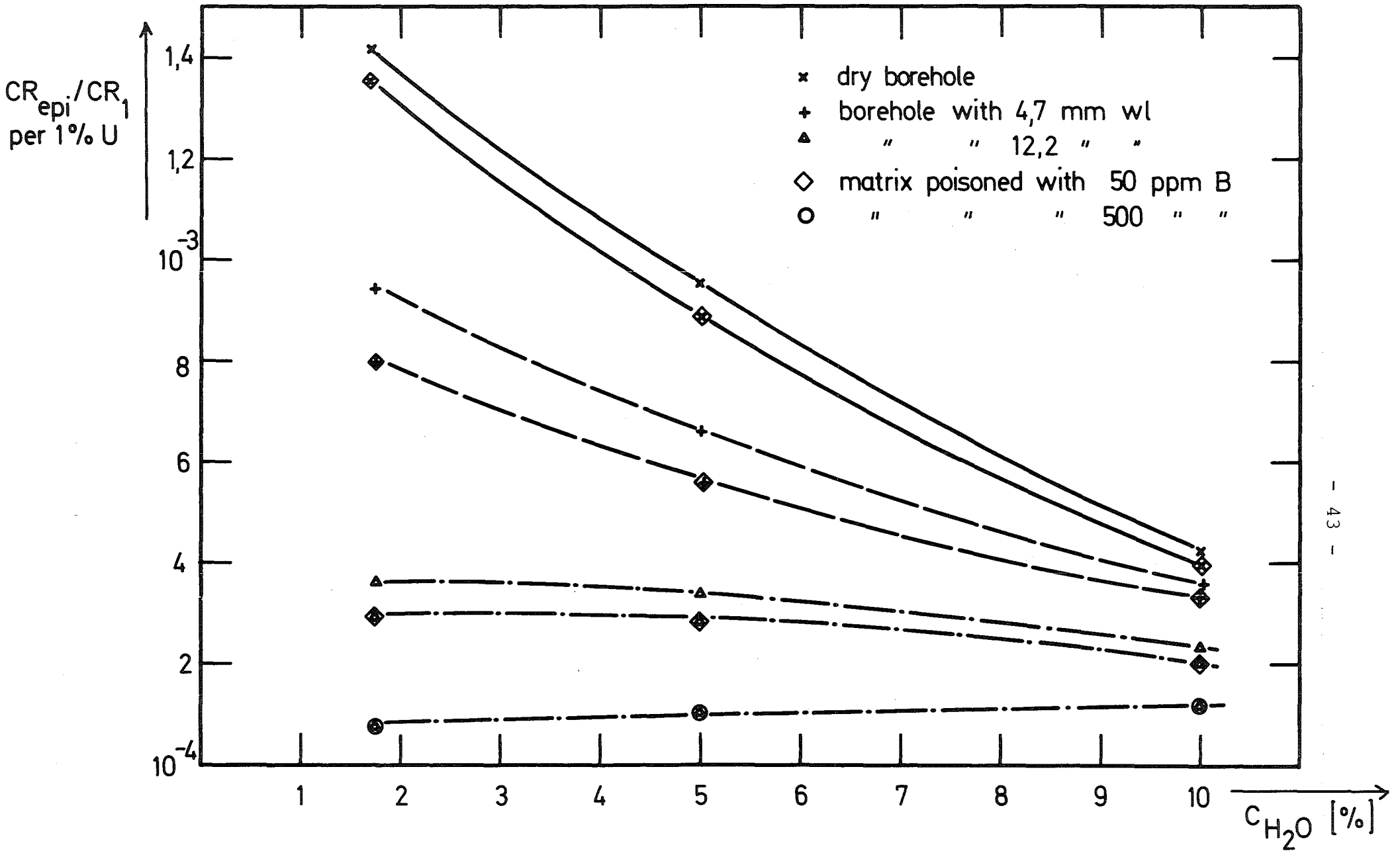

Fig. 15 Epithermal prompt fission neutron to total neutron countrate ratio as function of matrix composition and borehole configuration

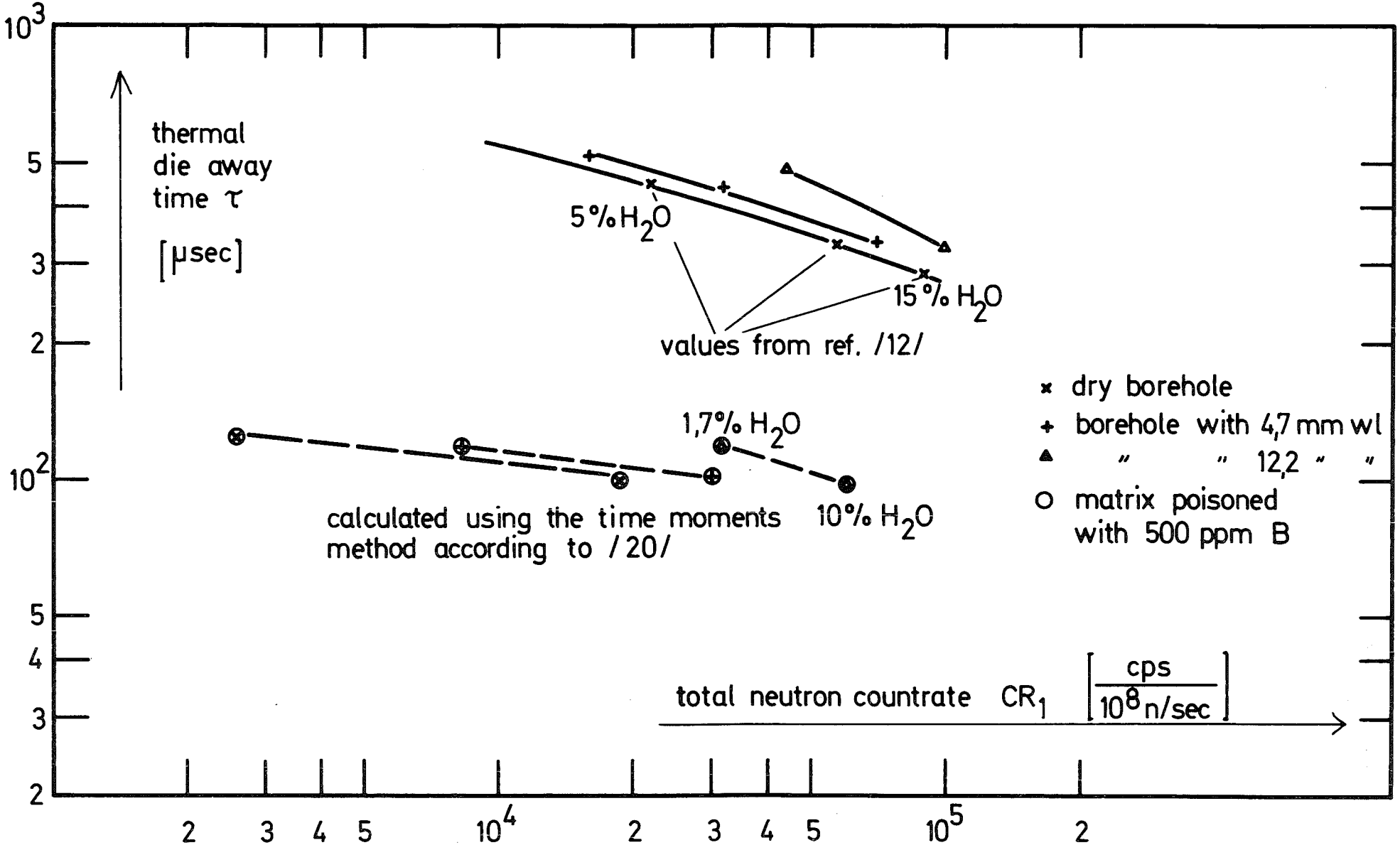

Fig. 16 Thermal neutron die away time τ for different matrix composition and borehole configuration